Monatshefte für Chemie 137, 1027–1042 (2006)
DOI 10.1007/s00706-006-0511-3

Monatshefte für Chemie
Chemical Monthly
Printed in Austria

Spectroscopic and Quantum Mechanical Studies of Substituted Anilines and their Charge-Transfer Complexes with Iodine in Different Solvents

Tarek M. El-Gogary[1,*], **Mostafa A. Diab**[2], and **Shreen F. El-Tantawy**[2,‡]

[1] Teacher's College in Jazan, Abo Areesh, Saudi Arabia
[2] Faculty of Science (Domyat), Mansoura University, Domyat Al-Gideda, Egypt

Received September 1, 2005; accepted November 8, 2005

Summary. Equilibrium constants and molar extinction coefficients for 1:1 charge-transfer complexes between 2-hydroxyaniline (*HA*), 5-chloro-2-hydroxyaniline (*CHA*), and 4-bromo-2,6-dimethylaniline (*BMA*) as donors and iodine, as a typical σ-acceptor were determined spectrophotometrically in chloroform, dichloromethane, and carbontetrachloride solutions. Spectral characteristics and formation constants are discussed in terms of donor molecular structure and solvent polarity. The stoichiometry of the complexes was established to be 1:1. For this purpose, optical data were subjected to the form of the *Rose-Drago* equation for 1:1 equilibria. Electronic absorption spectra of the studied anilines were measured in different solvents. Spectral data were reported and band maxima were assigned to the appropriate molecular orbital transitions (π–π^* and n–π^* electronic transition). Solvent effects on the electronic transitions were discussed. Optimized geometry of the studied anilines was obtained at B3LYP/6-31 + G(d). The effect of the electronic factors of the substituents on the geometrical parameters of the ring has been explored. Geometrical values of the ring deviate from the regular hexagonal ring. Intramolecular H-bonds in *HA* and *CHA* have been computed at B3LYP/6-31 + G(d) and MP2/6-31 + G(d) levels. The H-bonding distance was calculated to be 2.105 Å in *HA* and 2.127 Å in *CHA*.

Keywords. Charge transfer complexes; Solvent effect; Electronic spectra; Geometry optimization; H-bond, intramolecular.

Introduction

Intermolecular charge-transfer (CT) complexes are formed when electron donors (D) and electron acceptors (A) interact [1]. *Mulliken* [2] considered such complexes to arise from a *Lewis* acid–*Lewis* base type of interaction, the bond between the components of the complex being postulated to arise from the partial transfer of

---

[*] Corresponding author. E-mail: tarekelgogary@yahoo.com

[‡] Abstracted from her M.Sc. thesis

π-electrons from the base (D) to orbitals of the acid (A). In solution, the composition of the complexed species could be represented by a 1:1 molar ratio [3], and the association equilibrium may be presented as:

$$\mathrm{D} + \mathrm{A} \xrightleftharpoons{K_{\mathrm{DA}}} \mathrm{D} - \mathrm{A}$$

A characteristic feature of a D–A complex is the appearance of a new absorption band in the spectrum of the complex, commonly attributed to an intermolecular CT transition, involving electron transfer from the donor to the acceptor. The term "CT complex" is misleading in that very little charge is actually transferred in the ground state for such complexes [4]. The nature of intermolecular CT complexes has been the subject of many investigations. Early work in this field was based mainly on *Mulliken*'s valence bond theory [2] in which the D–A complex is described as a resonance hybrid of an uncharged aggregate (D,A), the so called 'no-bond' state and an ionic 'dative' state (D^{+}–A^{-}) formed by charge transfer from D to A. This theory was able to provide an adequate explanation of many spectroscopic results and to predict the most stable complex geometries. However, it is not sufficient to consider only CT interactions when describing the properties of the complexes in which this interaction is not the dominant contribution to the ground-state stabilization. More detailed theoretical studies [5–7] indicated that contributions from different types of interactions (electrostatic, charge-transfer, steric, exchange repulsion, and polarization) are all important. Experimental results also suggested that the D–A partners at close separation are held together mainly by *van der Waals*-type forces [8].

Aniline is the precursor of a large set of molecules of biological and pharmacological interest. Biochemical studies on aniline and many of its derivatives showed that these compounds represent important biochemical active substances. They have many applications in both human and veterinary medicine [9]. The most important uses of aniline are in the manufacture of dyes and rubber chemicals. It has some importance as corrosion inhibitor. It appears to be especially suitable for protecting some metal against wet corrosion of carbontetrachloride. Some amount of aniline is used in the textile, paper, and metallurgical industries, and as catalyst as, stabilizers, pesticides, and insect and animal repellents too. It is also used as a solvent and analytical reagent. In the pharmaceutical industry, aniline is important in the manufacture of sulpha drugs and synthetic sweetening agents.

Following these widespread applications of anilines in industry and medicine, we have studied spectrophotometrically 2-hydroxy aniline (*HA*), 5-chloro-2-hydroxy aniline (*CHA*), and 4-bromo-2,6-dimethylaniline (*BMA*).

Anilines and its derivatives have considerable donor strength but as donor molecules, they can't be classified into either n- or π-donors because the lone pair orbital electrons on the nitrogen atom of the amine group involve in conjugation with the π-orbitals of the benzene ring. The donor properties of the anilines increase when an electron releasing group is introduced either on the nitrogen atom or in the benzene ring. For that anilines have been widely used as donors with different acceptors in many charge-transfer complexation studies. *Budni et al.* [10] have investigated spectrophotometrically molecular complexes of 2,3,5,6-tetrachloro-7-nitro-1,4-naphthoquinone with aromatic anilines in carbontetrachloride. *Kumar et al.* [11]

have studied molecular complexes of *DDQ* with aniline, spectrophotometrically, by stabilizing the complexes in a low polar solvent (CCl_4), at low temperatures, and under low donor concentrations. Complexation between *o*-chloranil and a series of anilines have been studied spectrophotometrically at room temperature [12]. *Bugeanu* and *Sachini Em* [13] calculated the stability constants and dipole moments of aniline complexes with iodine acceptor by different methods. The visible spectra of some molecular complexes of aromatic primary amines with iodine have been recorded in chlorine-containing aliphatic solvents [14]. The formation of charge-transfer complexes between iodine and aniline, *N*,*N*-dimethylaniline, 2,6-dimethylaniline, and 2,4,6-trimethylaniline in $CHCl_3$, CH_2Cl_2, CH_2Cl_2:$CHCl_3$ (1:1), and CH_2Cl_2 have been studied by *Kwon et al.* [15]. The ultra-violet and visible absorption spectra of the complexes of iodine and aniline have been reported by *Kusakawa* and *Nishizaki* [16]. *Andrabi* [17] has determined the formation of yellow colored charge-transfer complexes of aniline, *N*-methylaniline, *N*,*N*-dimethylaniline, and *N*,*N*-diethylaniline with nitromethane in carbontetrachloride by UV-VIS spectrophotometry. The equilibrium constant for complexation of C60 and aniline in toluene measured by *Sibley et al.* [18] and the absorption spectra of the complexation of fullerene C70 with aniline were obtained [19]. The UV spectrum of *p*-nitroaniline [20], *m*-nitroaniline [21], acetoacetanilide, benzoylacetanilide [22], and various para-substituted benzylidene aniline molecules at room temperature [23] have been studied. *Aly et al.* [24] have studied the spectroscopic and thermodynamic behavior of the charge-transfer complexes between 4-([2,2]paracyclophanoyl)amines and π-acceptors.

Ying and *Hong* [25] have studied the spectral and thermodynamic behavior of the charge-transfer complexes formed by vitamin K_1, K_3 and N-substituted anilines. *Pal et al.* have investigated charge-transfer complexes of menadione (vitamin K_3) with a series of anilines [26].

In the present study, charge-transfer complexes of 2-hydroxy aniline (*HA*), 5-chloro-2-hydroxy aniline (*CHA*), and 4-bromo-2,6-dimethylaniline (*BMA*) with iodine, as a typical σ-acceptor, are studied spectrophotometrically in chloroform, dichloromethane, and carbontetrachloride solutions. Electronic absorption spectra of the studied anilines were measured in different solvents and assigned to their proper electronic transitions. Geometry of the studied anilines are obtained at B3LYP/6-31 + G(d). The effect of electronic factors of the substituents on geometrical parameters of the ring has been explored.

Results and Discussion

Geometrical Structures

Up to our knowledge no *ab initio* and DFT calculations have been performed on *HA*, *CHA*, and *BMA* molecules. The aim of this study is to calculate optimal molecular geometry, and strength of the intramolecular H-bond in *HA*. The optimized structures of *HA*, *CHA*, and *BMA* calculated at *ab initio* DFT B3LYP level with the 6-31G(d) basis set are listed in Table 1 in accordance with the atom numbering scheme given in Fig. 1. Our calculated results show that the aromatic ring in *HA*, *CHA*, and *BMA* is distorted, compared to the regular hexagon, due to steric and

Table 1. Solution of aniline compounds in different solvents with their stock concentrations, measured concentrations, and wavelength regions of measurment

Solution	Stock conc. (*M*)	Measured conc. (*M*)	Wavelength region (nm)
BMA/CCl_4	8.995×10^{-4}	4.32×10^{-4}	450–265
BMA/CH_2Cl_2	2.490×10^{-2}	2.49×10^{-4}	450–232
BMA/$CHCl_3$	1.080×10^{-3}	4.10×10^{-4}	450–250
BMA/*Et*OH	1.320×10^{-3}	1.06×10^{-4}	450–210
BMA/*Me*OH	1.199×10^{-3}	9.59×10^{-5}	450–210
BMA/CH_3CN	1.880×10^{-3}	7.52×10^{-5}	450–210
BMA/*DMF*	1.880×10^{-3}	3.01×10^{-4}	450–270
CHA/CCl_4	4.179×10^{-4}	2.01×10^{-4}	500–265
CHA/CH_2Cl_2	2.400×10^{-3}	2.40×10^{-5}	500–232
CHA/$CHCl_3$	1.030×10^{-3}	3.09×10^{-4}	500–250
CHA/*Et*OH	1.920×10^{-3}	1.54×10^{-4}	500–210
CHA/*Me*OH	2.340×10^{-3}	2.81×10^{-4}	500–210
CHA/CH_3CN	2.620×10^{-3}	2.10×10^{-4}	500–210
CHA/*DMF*	1.090×10^{-3}	1.74×10^{-4}	500–270
HA/CCl_4	6.230×10^{-4}	2.99×10^{-4}	500–265
HA/CH_2Cl_2	1.060×10^{-4}	1.06×10^{-4}	500–232
HA/$CHCl_3$	1.060×10^{-3}	2.12×10^{-4}	500–250
HA/*Et*OH	1.690×10^{-3}	1.35×10^{-4}	500–210
HA/*Me*OH	2.460×10^{-3}	2.95×10^{-4}	500–210
HA/CH_3CN	1.980×10^{-3}	1.58×10^{-4}	500–210
HA/*DMF*	1.650×10^{-3}	2.64×10^{-4}	500–270

electronic effects of electron donating and electron withdrawing substituents in the ring. Since large deviations from experimental C–H bond lengths may arise from the low scattering factors of hydrogen atoms in the X-ray diffraction experiment we are not going to discuss C–H bond lengths. The B3LYP method leads to geometric parameters which agree well to experimental data. For that we take into account B3LYP/6-31G(d) level for studying the geometry of *HA*, *CHA*, and *BMA* in the present work. To the best of our knowledge, experimental data on the geometric structure of *HA*, *CHA*, and *BMA* are not available in the literature. Therefore, we could only compare the calculation results given in Table 1 with the experimental data of *p*-methylaniline [27]. The optimized geometric parameters (bond lengths and angles) at B3LYP/6-31G(d) are listed in Table 2 and are compared with the experimentally determined geometry parameters for *p*-methylaniline [38]. The optimized parameters obtained by the various methods are fairly similar. Several authors [28–32] explained the changes in bond length of the C–H bond on substitution due to a change in the charge distribution on the carbon atom of the benzene ring. The substituents may be either of the electron withdrawing type (Cl, Br) or electron donating type (CH_3, C_2H_5). The carbon atoms are bonded to the hydrogen atoms with a σ bond in benzene and the substitution of a halogen for a hydrogen reduces the electron density at the ring carbon atoms. The ring carbon atoms in substituted benzenes exert a larger attraction on the valence electron cloud of the hydrogen atom resulting in an increase in the C–H force constant and a corresponding decrease in the bond length. The reverse holds true on substitution with electron

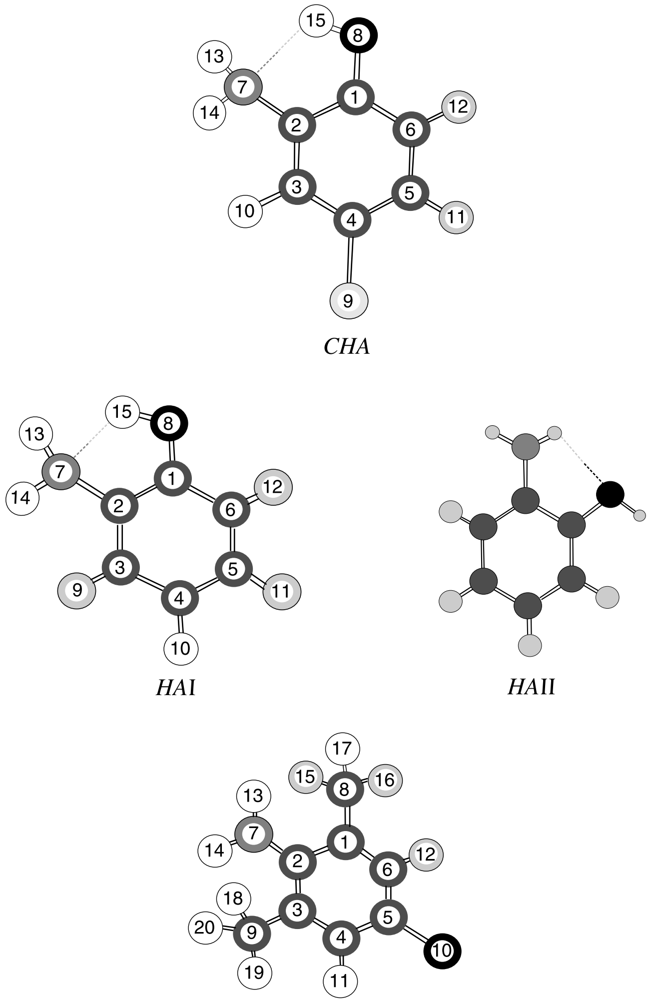

CHA

*HA*I

*HA*II

BMA

Fig. 1. Optimized structures of the studied aniline derivatives showing intramolecular H-bond (in *HA*) and atomic numeration

donating groups. The actual change in the C–H bond length would be influenced by the combined effects of the inductive-mesomeric interaction and the electric dipole field of the polar substituent. With respect to the experimental data for aniline and its derivatives [33–35] one can see in Table 1 that most of the bond lengths are underestimated. The amino nitrogen atom, in *HA* and *CHA* is slightly out of plane, with a torsional angle C4–C3–C2–N in the range of 178–179° (or about 1–2°) while in *BMA* the amino N atom lies in the ring plane, with a torsional angle C4–C3–C2–N, 180°. A measure of this displacement is known as the tilt angle [36]. Existence of this angle has been interpreted to be caused by asymmetric interaction between the NH_2 group and benzene ring plane. This interaction is common to all aniline derivatives [37, 38]. C2–N distances in *HA* (1.4387 Å) and in *CHA* (1.4342 Å) are similar to the distances for aniline (measured 1.402 and calculated 1.407 Å) [39] and for *p*-methylaniline (measured 1.43 and calculated 1.414 Å) [27]. In *HA* and *CHA*, the C1–C2 bond is found to be longer than the C2–C3 bond of the ring

Table 2. Calculated geometrical parameters of *BMA*, *HA*, and *CHA* and experimental geometrical data of *p*-methylaniline

	BMA	*HA*		*CHA*		Exp. *p*-methylaniline	
Bond length		Bond length		Bond length		Bond lengths	
C1–C2	1.4136	C1–C2	1.4079	C1–C2	1.4077	C1–C2	1.36
C1–C6	1.4001	C1–C6	1.398	C1–C6	1.3971	C1–C6	1.40
C1–C8	1.5055	C1–O	1.3584	C1–O	1.3582		
C2–C7	1.3835	C2–C3	1.3994	C2–C3	1.3991	C2–C3	1.39
C4–C5	1.396	C2–N	1.4387	C2–N	1.4342	C2–N	1.43
C4–C11	1.0876	C3–C4	1.3995	C3–C4	1.397	C3–C4	1.40
C5–Br	1.9006	C3–H9	1.089	C3–H10	1.0878	C3–H9	1.08
N–H13	1.003	C4–C5	1.4014	C4–C5	1.3982	C4–H10	1.08
C–H (methyl)[a]	1.095	C4–H10	1.0866	C4–Cl	1.7395		
Bond angle		C5–C6	1.3978	C5–C6	1.3974		
C2C1C6	119.4517	C5–H11	1.0872	C5–H11	1.0862	C5–C6	1.39
C2C1C8	119.9171	C6–H12	1.0868	C6–H12	1.0866		
C6C1C8	120.6312	N–H13	1.0153	N–H13	1.0155		
C1C2C3	120.102	N–H14	1.0131	N–H14	1.0129	N–H14	1.02
C1C2N	119.9528	O–H15	0.9738	O–H15	0.9733		
C3C2N	119.9452	Bond angle		Bond angle			
C2C3C4	119.4261	C2C1C6	120.3003	C2C1C6	120.0555		
C2C3C9	119.9448	C2C1O	119.8329	C2C1O	119.9802		
C4C3C9	120.6291	C6C1O	119.8513	C6C1O	119.9356	C2–C1–C6	120.5
C3C4C5	120.2388	C1C2C3	119.5253	C1C2C3	119.7748	C3–C4–C5	121.5
C3C4H11	119.6381	C1C2N7	115.2951	C1C2N	115.524	C3–C4–H10	119.2
C5C4H11	120.1231	C2C3C4	120.3153	C2C3C4	119.5312	C5–C4–C9	120.3
C4C5C6	120.5628	C2C3H9	119.2403	C2C3H10	120.2026	C1–C2–N	109.5
C4C5Br	119.7206	C4C3H9	120.3922	C4C3H10	120.1604	C2–C3–C4	120.5
C6C5Br	119.7166	C3C4C5	119.6209	C3C4C5	120.7929	C4–C3–H9	120.5
C1C6C5	120.2186	C3C4H10	120.0075	C3C4Cl	119.3027	C1–C2–C3	109.5
C1C6H12	119.6459	C5C4H10	120.3513	C5C4Cl	119.8264	C2–C3–N	109.5
C5C6H12	120.1354	C4C5C6	120.5632	C4C5C6	119.5876		
C2NH13	121.4368	C4C5H11	119.9873	C4C5H11	119.9397	H13–N–H14	113.0
C2NH14	121.4333	C6C5H11	119.4354	C6C5H11	120.4348		
H13NH14	117.1299	C1C6C5	119.5655	C1C6C5	120.0486		
C1C8H15	111.4234	C1C6H12	118.8964	C1C6H12	119.0225		
C1C8H16	110.8987	C5C6H12	121.4813	C5C6H12	120.8166		
C1C8H17	111.4236	C2NH13	111.8620	C2NH13	111.9583		
H15C8H16	107.6108	C2NH14	111.5548	C2NH14	111.8232		
H15C8H17	107.6882	H13N7H14	108.0778	H13NH14	108.2653		
H16C8H17	107.6106	C1OH15	105.4688	C1OH15	105.7899		
C1C2NH13	0.0362	C1C2NH13	100.3256	C1C2NH13	94.5224		
C3C2NH13	179.98	C3C2NH13	83.6654	C1C2NH14	143.777		
NC2C3C4	180.00	NC2C3C4	178.9552	NC2C3C4	179.0503		

[a] Average

by 0.065 Å. However, in *MBA* these two bonds are the same due to the symmetry of the molecule. The C–Br bond calculated to be 1.9005 Å in *BMA* where the C–Cl bond length is found to be 1.7395 Å which is similar to that calculated for 3-chloro-4-methylaniline [40]. The C1–C2–C3 and C3–C4–C5 angles in *BMA* are calculated to be 120.102 and 120.2388°, respectively, which are larger than the typical hexagonal angle of 120°. The C4–C5–C6 angle is found to be about 0.56° larger than the normal hexagonal angle. Similar values were reported for other aniline derivatives; *m*-methylaniline [41], *o*-methylaniline [42], and *p*-methylaniline [27].

Intramolecular H-bonding in *HA* and *CHA* has been investigated by means of quantum mechanical calculations at B3LYP/6-31 + G(d). It is well known that intramolecular H-bond is much weaker than the intermolecular one as a result of the molecular geometry strain. Intramolecular H-bond in *HA* is stronger than that in *CHA* as suggested by the intramolecular H-bond distance which is found to be

2.105 Å in *HA* and to 2.127 Å in *CHA*. This can be attributed to the effect of the chlorine atom which, as an electron withdrawing species, reduces the electron density in the ring and in turn at the amino nitrogen atom. This leads to the elongation of the N···H hydrogen bond. This argument is evidenced with the shorter C–N distance (higher double bond character), 1.4342 Å in *CHA* compared to 1.4387 Å in *HA*. Two possible intramolecular H-bonds could be formed in *o*-hydroxyanilines by changing the torsion angle C6–C1–O8–H15. In the first one the hydroxy group will be the H-bond donor and the amino nitrogen will be the H-bond acceptor (*HA*I) while in the second one (*HA*II) the reverse is true. Both structures have been studied and optimized at B3LYP/6-31 + G(d) and MP2/6-31 + G(d) levels for *HA* and are presented in Fig. 1. The B3LYP calculation results show that *HA*I is more stabilized by 4.839 kJ/mol than *HA*II and MP2 has confirmed the extra stabilization of *HA*I compared to *HA*II by 1.901 kJ/mol. This is also evidenced by the H-bonding distance calculated to be 2.105 Å in *HA*I compared to 2.279 Å in *HA*II. However, both values of energies are small to allow the coexistence of the two conformers. The stabilization energy calculated at MP2 level is less than half of that calculated at B3LYP level because the MP2 method is accounting for the electron correlation effects much more than the B3LYP method does. This also indicates that the intramolecular H-bonding is mainly affected by electronic effects.

Electronic Spectra of Aniline Compounds

The electronic absorption spectra of *HA*, *CHA*, and *BMA* were measured in CCl_4, CH_2Cl_2, $CHCl_3$, *Me*OH, *Et*OH, CH_3CN, and *DMF*. The observed spectra for *BMA*, as a representative example, in these different solvents are given in Fig. 2. The observed UV-VIS spectra showed two absorption bands as a result of two electronic

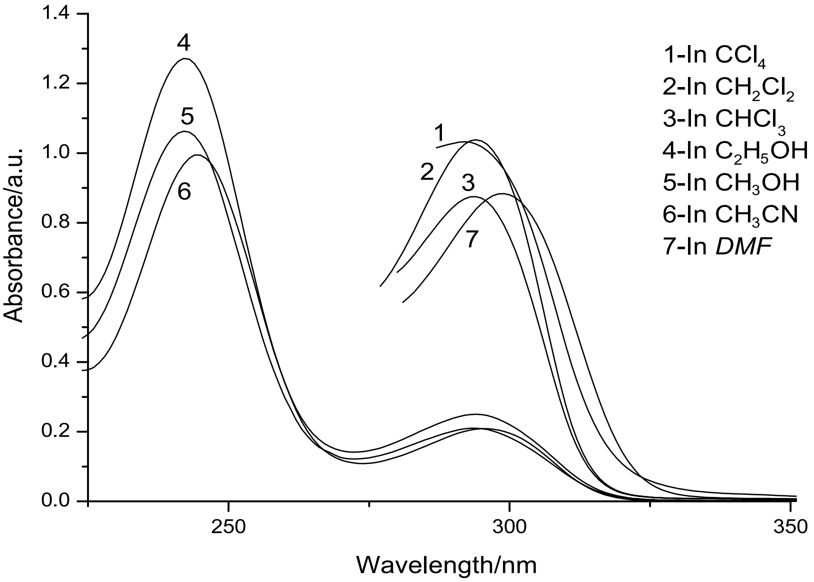

Fig. 2. The observed UV-VIS spectra of 4-bromo-2,6-dimethylaniline in different solvents at room temperature

transitions (π–π^* and n–π^* transitions). The intensities of these observed bands were estimated by determining the *Einstein* transition probability coefficients of emission (A_{if}) and absorption (B_{if}) and the half life time of the excited states of the observed transitions. Determination of absolute intensity of an absorption band is well explained by *Sandorfy* [43]. The *Einstein*'s transition probability coefficients of emission (A_{if}) and absorption (B_{if}) between two, initial (i) and final (f), electronic states are given by Eqs. (1) and (2).

$$A_{\mathrm{if}} = \frac{64\pi \overset{-3}{\upsilon} e^2}{3h} G_{\mathrm{f}}\, D_{\mathrm{if}} \tag{1}$$

$$B_{\mathrm{if}} = \frac{8\pi^3 e^2}{3h^2 c} G_{\mathrm{f}}\, D_{\mathrm{if}} \tag{2}$$

e: charge of electron, h: *Planck*'s constant, υ: frequency of radiation (cm^{-1}),
c: velocity of light, G_{f}: degeneracy of the final state, D_{if}: dipole strength.

By substituting the known numerical values in Eqs. (1) and (2) and by assuming that degeneracy of the state is unity one gets Eqs. (3) and (4).

$$A_{\mathrm{if}} = 7.24\times 10^{10}\, \overset{-3}{\upsilon}\, D_{\mathrm{if}} \tag{3}$$

$$B_{\mathrm{if}} = 14.5\times 10^{24} D_{\mathrm{if}} \tag{4}$$

Numerically D_{if} [54] is given by Eq. (5).

$$D_{\mathrm{if}} = 3.98\times 10^{-20} \frac{1}{\upsilon} \int \varepsilon(\upsilon) d\upsilon \tag{5}$$

The integral $\int \varepsilon(\upsilon) d\upsilon$ is the area of the absorption band; *Gaussian* analysis gives such area by Eq. (6).

$$\int \varepsilon(\upsilon) d\upsilon = \varepsilon_{\max}(1.0645)h \tag{6}$$

where h is the half-width of the absorption band in cm^{-1}. With the value given in Eq. (4) the oscillator strength f is given by Eq. (7) and the life time of the exited state is then given by Eq. (8).

$$f = 4.6\times 10^{-9} \varepsilon_{\max} h \tag{7}$$

$$\tau = 1/A_{\mathrm{if}} \tag{8}$$

The observed values of $\lambda_{\max}$ with their molar extinction coefficients and estimated probability coefficients, half life time, and oscillator strengths (f) are tabulated in Table 3. The transition probabilities A_{if} and B_{if} for the observed transitions have values in the order of 10^6 which are large enough to indicate the allowance of these transitions. Life times of the excited state are of the order of 10^{-8} s which is evidence that these transitions are allowed. The lower energy band (Band I) was observed between 287 and 432 nm and showed a general low intensity character ($\varepsilon = 2.13\times 10^3$–$4.32\times 10^3$ dm^3 mol^{-1} cm^{-1}). This indicates that this absorption band is attributed to a kind of n → π^* electronic transition between the lone pair

Table 3. Spectral characteristics of the observed bands of 4-bromo-2,6-dimethylaniline, 2-hydroxyaniline (between brackets), and 5-chloro-2-hydroxyaniline (*italic*); their bands maxima (λ_{max}), molar extinction coefficients (ε), *Einstein*'s probability coefficients, oscillator strengths (*f*), and life time of the excited state in different solvents

Solvent	$\frac{\lambda_{max}}{nm}$	$\frac{\varepsilon_{max}\times10^{-3}}{dm^3\ mol^{-1}\ cm^{-1}}$	Probability coefficients		Oscillator strength *f*	Life time $\tau\times10^8$ s
			Emission $A_{if}\times10^{-6}\ s^{-1}$	Absorption $B_{if}\times10^{-6}$ s/g		
CCl_4	293	2.37	31.277	157.976	0.04337	3.197
	(414)	(0.177)	(12.877)	(181.974)	(0.00329)	(7.766)
	(287)	(2.88)	(54.108)	(256.516)	(0.06703)	(1.837)
	425	*0.328*	*26.059*	*402.138*	*0.00707*	*3.838*
	298	*4.95*	*57.253*	*304.998*	*0.07651*	*1.746*
$CHCl_3$	294	2.13	21.752	110.838	0.02822	4.597
	(290)	(4.32)	(45.108)	(220.002)	(0.05683)	(2.216)
	432	*0.181*	*84.137*	*136.704*	*0.00236*	*1.188*
	298	*3.22*	*28.487*	*151.754*	*0.03807*	*3.510*
CH_2Cl_2	295	4.14	40.863	210.066	0.05332	2.447
	(289)	(2.77)	(29.498)	(142.626)	(0.03695)	(3.390)
	(236)	(6.49)	(14.995)	(393.994)	(0.12508)	(6.669)
	297	*5.38*	*53.976*	*282.450*	*0.07127*	*1.853*
	241	*10.30*	*22.418*	*628.179*	*0.19521*	*4.461*
Ethanol	295	2.28	23.629	121.473	0.030834	4.232
	243	12.0	26.367	755.080	0.23294	3.793
	(287)	(3.21)	(32.195)	(152.998)	(0.03986)	(3.106)
	(234)	(6.78)	(16.675)	(438.122)	(0.13909)	(5.997)
	298	*4.05*	*38.008*	*200.669*	*0.05048*	*2.631*
	240	*6.99*	*15.731*	*440.794*	*0.13697*	*6.356*
Methanol	295	2.15	22.964	118.053	0.02997	4.355
	243	11.0	24.341	967.078	0.21505	4.108
	(287)	(2.83)	(29.330)	(139.382)	(0.03632)	(3.409)
	(234)	(5.85)	(13.904)	(355.181)	(0.11382)	(7.191)
	297	*3.63*	*36.419*	*190.575*	*0.04809*	*2.746*
	240	*6.19*	*13.734*	*384.847*	*0.11959*	*7.281*
CH_3CN	297	2.74	24.817	129.865	0.32770	4.029
	245	13.2	27.297	804.944	0.24592	3.663
	(291)	(3.36)	(33.102)	(164.288)	(0.04219)	(3.021)
	(238)	(7.78)	(15.028)	(406.252)	(0.12776)	(6.654)
	299	*3.83*	*37.220*	*200.063*	*0.05004*	*2.687*
	244	*6.88*	*12.700*	*369.049*	*0.11329*	*7.873*
DMF	299	2.91	29.674	159.499	0.03989	3.370
	(295)	(4.01)	(38.635)	(198.613)	(0.05041)	(2.588)
	303	*4.22*	*37.637*	*209.752*	*0.05183*	*2.657*

of the N-atom and the benzene ring moieties. Such a transition can be considered as a kind of intramolecular charge transfer between nitrogen atom and benzene ring. As observed from Table 3 the spectra of concerned molecules in different solvents with different polarities showed that this band was slightly shifted to lower wavelength with increasing solvent polarity which characterizes its nature as an $n \rightarrow \pi^*$ transition band. The second band (Band II), which is the higher energy one was detected between 234 and 245 nm and showed intensities in the range $\varepsilon = 2.88 \times 10^3 – 13.00 \times 10^3\ \mathrm{dm^{-3}\ mol^{-1} cm^{-1}}$. This indicates that we are dealing with an absorption band due to $\pi \rightarrow \pi^*$ transition as a result of the π-system of the benzene ring. This transition was shifted to longer wavelength with increasing solvent polarity which characterizes its nature as a $\pi \rightarrow \pi^*$ transition.

Intermolecular Charge-Transfer Complexes of Aniline-Iodine Complexes

In this part, an attempt is made to investigate the nature of the charge-transfer complexes of aniline compounds as donors with iodine as acceptor. This investigation was carried out spectrophotometrically in three different solvents chloroform, dichloromethone and carbontetrachloride, at room temperature. Thus the solvent effect on the equilibrium constants of the formed charge-transfer complexes was studied.

Some typical CT absorption spectra of the mixtures of *HA* with iodine are given in Fig. 3. When the mixture of donor and acceptor solutions gives rise to a spectrum which is not due to the components of the mixture, the absorption peak at longer wavelength is identified as charge transfer band. The CT bands for BMA/I_2 are observed at $\lambda_{max} = 352$, 352, and 358 nm in chloroform, dichloromethane, and carbontetrachloride, respectively (Table 3), while HA/I_2 shows CT bands at $\lambda_{max} = 361$, 362, and 367 nm, and CHA/I_2 gives CT transitions at $\lambda_{max} = 362$, 363,

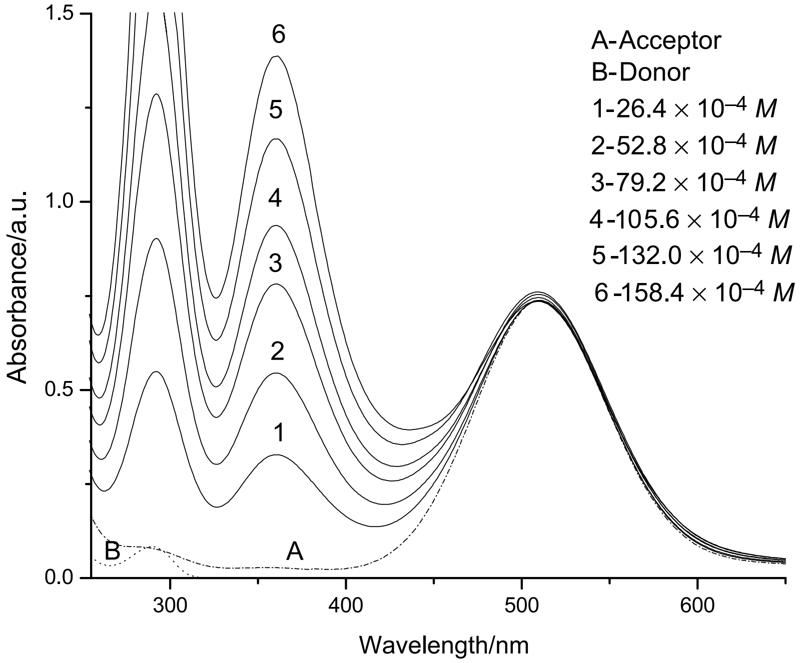

Fig. 3. Absorption spectra of pure iodine (A) ($8.16 \times 10^{-4}\,M$), pure 2-hydroxyaniline (B) ($26.4 \times 10^{-4}\,M$) and their mixed solutions in chloroform at room temperature

Table 4. The characteristic data of the charge-transfer complexes of iodine-donor mixed solution in different solvents at room temperature

Donor	Solvent	CT band		Position of isosbestic point (nm)	Stability constant K_{DA}
		$\frac{\lambda_{max}}{nm}$	$\frac{\varepsilon_{max}}{dm^3\ mol^{-1}\ cm^{-1}}$		
BMA	$CHCl_3$	352	6087	–	10.3 ± 0.1
	CH_2Cl_2	352	6916	–	11.0 ± 0.1
	CCl_4	358	5401	–	11.4 ± 0.1
HA	$CHCl_3$	361	2573	476	71.9 ± 1.7
	CH_2Cl_2	362	2164	477	73.8 ± 1.8
	CCl_4	367	1250	–	74.9 ± 2.0
CHA	$CHCl_3$	362	1303	464	84.4 ± 2.1
	CH_2Cl_2	363	1161	465	85.4 ± 2.1
	CCl_4	439	9692	–	86.3 ± 2.3

and 439 nm (Table 4). The CT bands are shifted to lower wavelength with increasing solvent polarity. According to *Mulliken*'s theory [2], the ground state of the complex is a resonance hybrid of a 'no-bond' state ($D\cdots A$) and a 'dative' state ($D^+\cdots A^-$) with the former predominating in typical loose complexes; the excited state is a resonance hybrid of the same two structures with the dative one predominating. This indicates that the polar solvent stabilizes the 'no-bond' state which is predominant in such systems.

Due to the fact that the *Benesi–Hildebrand* method [44] of analysis does not distinguish the CT-complexes stoichiometry, it is more appropriate to use the *Rose-Drago* [45] treatment which, however, distinguishes the species of 1:1 stoichiometry from others. Thus, the *Rose-Drago* method was used to calculate the stability constant K_{DA} and the molar extinction coefficient (ε) of the complexes. For all the systems of iodine with various aromatic anilines, good linear plots were obtained from the *Rose-Drago* method, which characterizes the existence of 1:1 stoichiometric species. Similar patterns were observed for all solvents, indicating that the stoichiometry of the complexes is 1:1 and is unaffected by change in the dielectric constant of the medium. The representative *Rose-Drago* linear plot obtained for one of the systems is shown in Fig. 4. The values of formation constants and molar extinction coefficients were calculated using such plots and are given in Table 4.

Of the three donors studied, *BMA* appears to be the weakest due the weak electron repelling effect of the Br atom and low positive hyperconjugative effect of the two methyl groups [46]. In addition to that the steric hindrance caused by the bulky methyl groups and the large-sized bromine atom should play a considerable negative role resisting the association between donor and acceptor moieties. *HA* shows higher formation constants and *CHA* the highest (Table 4). This can be attributed to the effect of the additional chlorine atom that has a strong positive mesomeric effect. The relative order of donor strength, based on the magnitudes of K_{DA} values, was found to be: *CHA* > *HA* > *BMA*. This order can be interpreted in the light of the electronic and steric effects derived from the substituent groups in the aromatic ring as discussed above.

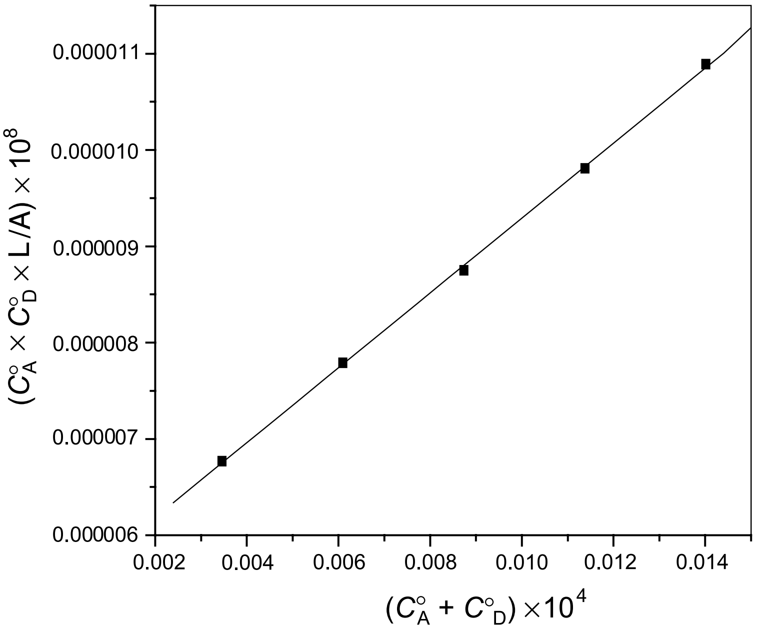

Fig. 4. *Rose-Drago* relation between $(C^{o}_{A} \times C^{o}_{D} \times L/A)$ and $(C^{o}_{A} + C^{o}_{D})$ of 2-hydroxyaniline-Iodine/$CHCl_3$ system at $\lambda_{max} = 361$ nm

Effect of Solvent on the Charge-Transfer Complexes of Anilines with Iodine

Formation constants for *BMA*/iodine complex are 10.307, 10.968, and 11.381 in $CHCl_3$, CH_2Cl_2, and CCl_4, respectively. Consistently, *HA*/iodine complex has formation constants of 71.878, 73.759, and 74.946 and *CHA*/iodine complex has the magnitudes of 84.443, 85.445, and 86.253 in $CHCl_3$, CH_2Cl_2, and CCl_4, respectively (Table 4). The difference in K_{DA} values of the charge-transfer complexes in $CHCl_3$, CH_2Cl_2, and CCl_4 indicates that the formation of the complexes in the latter solvent is most favorable, most probably because the complexes formed are less polar than their components (donor and acceptor) individually [47, 48]. In a complex of a nonpolar donor with a nonpolar acceptor, the dipole moment of the no-bond structure will usually be very small and may be equal to zero. However, there will be a dipole moment associated with the dative bond structure and it will be directed from donor to acceptor. Since the actual ground state wave function of the complex is an admixture of both the no-bond and the dative bond wave functions, this implies there will be a dipole moment of the complex. In our case the donors have high dipole moments so we do expect that the formed complex would be less polar. This argument explains the higher stability constants of the complexes in the less polar solvent, carbontetrachloride (Table 4).

Conclusions

The geometrical data of the studied anilines were optimized at B3LYP/6-31 + G(d). The effect of the electronic factors of the substituents on the geometrical parameters of the ring has been explored. Geometrical values of the ring deviate from the regular hexagonal ring. Intramolecular H-bonds in *HA* and *CHA* have been computed at B3LYP/6-31 + G(d) and MP2/6-31 + G(d) levels. The H-bonding distance has been calculated to be 2.105 Å in *HA* and 2.127 Å in *CHA*. The iodine acceptor forms strong CT-complexes of 1:1 stoichiometry with a set of aromatic anilines in chloroform, dichloromethane, and carbontetrachloride. The stoichiometry of the complexes is unaltered by changing the dielectric constant of the medium. The formation constants, molar extinction coefficients, and spectroscopic parameters of the complexes were found to be highly solvent dependent.

Experimental

The solvents used throughout this work are carbontetrachloride, dichloromethane, absolute ethanol, methanol, acetonitrile, and dimethylformamide. These solvents were supplied by Fluka and purified by conventional methods reported in literature [49].

Crystalline samples of 2-hydroxyaniline, 4-bromo-2,6-dimethylaniline, and 5-chloro-2-hydroxyaniline were supplied by Sigma-Aldrich Chemical Company (99, 98, and 97% purity). Crystalline iodine was obtained as Analar Grade from MERCK Chemical Company. It was further purified by sublimation.

Stock solutions of iodine were prepared freshly before use. Iodine solutions in different solvents were prepared by weight and exact concentrations were checked by measuring its UV-VIS absorbance (520 nm, $\varepsilon = 960\,M^{-1}\,\mathrm{cm}^{-1}$ at room temperature).

Stock solutions of the aniline compounds were prepared by weight just before measurement to avoid air oxidation.

Electronic Spectra Measurements

Stock solutions of all compounds were prepared in different solvents. All UV-VIS spectroscopic measurements were obtained in different organic solvents diluted to appropriate concentrations (Table 1). The UV-VIS absorption spectra of solutions were generally measured according to the methods reported in literature [50, 51] using a PERKIN ELMER Lambda-2 UV-VIS spectrophotometer. A quartz cell, 1.0 cm path length, was used. The spectra were reproducible in all cases.

UV-VIS Measurements of Charge-Transfer Complexes

The charge-transfer complex solutions were generally prepared by mixing the donor- and the acceptor-solutions by accurate dilution from stock solutions. Mixtures were left for about 15 min to reach equilibrium and then recorded against the solvent as reference. The results were found to be highly reproducible. Stock solutions of donors and acceptors were prepared. Separate combinations of the stock solutions were made, each containing a fixed concentration of acceptor solution and different donor concentrations. Spectra of these mixtures and the pure individual components were recorded.

BMA–I_2/CCl_4: Stock solution of *BMA* (0.1519 g, $3.04\times10^{-2}\,M$) in carbontetrachloride (25 cm^3) and I_2 (0. 1983 g, $7.81\times10^{-3}\,M$) in carbontetrachloride (100 cm^3) were used. The following *BMA* + I_2 mixtures (in cm^3) were prepared: 1 + 1, 2 + 1, 3 + 1, 4 + 1, 5 + 1, and 6 + 1. UV-VIS spectra were obtained in the region (700–250 nm) against carbontetrachloride as a blank following the general method above using I_2 in carbontetrachloride ($7.8\times10^{-4}\,M$) and *BMA* in carbontetrachloride (3.04×10^{-3}, 6.08×10^{-3}, 9.12×10^{-3}, 12.16×10^{-3}, 15.2×10^{-3}, $18.24\times10^{-3}\,M$)

BMA–I_2/CH_2Cl_2: Stock solution of *BMA* (0.1248 g, $2.49\times10^{-2}\,M$) in dichloromethane (25 cm^3) and I_2 (0.2070 g, $8.16\times10^{-3}\,M$) in dichloromethane (100 cm^3) were used. The following *BMA* + I_2 mixtures (in cm^3) were prepared: 1 + 1, 2 + 1, 3 + 1, 4 + 1, 5 + 1, and 6 + 1. UV-VIS spectra were obtained in the region (700–232 nm) against dichloromethane as a blank following the general method above using I_2 in dichloromethane (8.16×10^{-4} *M*) and *BMA* in dichloromethane (2.49×10^{-3}, 4.98×10^{-3}, 7.47×10^{-3}, 9.96×10^{-3}, 12.45×10^{-3}, 14.94×10^{-3} *M*).

BMA–I$_2$/CHCl$_3$: Stock solution of *BMA* (0.1395 g, 2.8×10^{-2} *M*) in chloroform (25 cm^3) and I_2 (0. 2072 g, 8.16×10^{-3} *M*) in chloroform (100 cm^3) were used. The following $BMA + I_2$ mixtures (in cm^3) were prepared: $1+1$, $2+1$, $3+1$, $4+1$, $5+1$, and $6+1$. UV-VIS spectra were obtained in the region (700–250 nm) against chloroform as a blank following the general method above using I_2 in chloroform (8.16×10^{-4} *M*) and *BMA* in chloroform (2.8×10^{-3}, 5.6×10^{-3}, 8.4×10^{-3}, 11.2×10^{-3}, 14.0×10^{-3}, 16.8×10^{-3} *M*).

HA–I$_2$/CCl$_4$: Stock solution of *HA* (0.0164 g, 6.0×10^{-3} *M*) in carbontetrachloride (25 cm^3) and I_2 (0.1983 g, 7.81×10^{-3} *M*) in carbontetrachloride (100 cm^3) were used. The following $HA + I_2$ mixtures (in cm^3) were prepared: $1+1$, $3+1$, $4+1$, $5+1$, and $6+1$. UV-VIS spectra were obtained in the region (700–250 nm) against carbontetrachloride as a blank following the general method above using I_2 in carbontetrachloride (7.8×10^{-4} *M*) and *HA* in carbontetrachloride (6.0×10^{-4}, 18.0×10^{-4}, 24.0×10^{-4}, 30.0×10^{-4}, 36.0×10^{-4} *M*).

HA–I$_2$/CH$_2$Cl$_2$: Stock solution of *HA* (0.0186 g, 6.8×10^{-3} *M*) in dichloromethane (25 cm^3) and I_2 (0.2070 g, 8.16×10^{-3} *M*) in dichloromethane (100 cm^3) were used. The following $HA + I_2$ mixtures (in cm^3) were prepared: $1+1$, $2+1$, $3+1$, $4+1$, $5+1$, and $6+1$. UV-VIS spectra were obtained in the region (700–232 nm) against dichloromethane as a blank following the general method above using I_2 in dichloromethane (8.16×10^{-4} *M*) and *HA* in dichloromethane (6.8×10^{-4}, 13.6×10^{-4}, 20.4×10^{-4}, 27.2×10^{-4}, 34.0×10^{-4}, 40.8×10^{-4} *M*).

HA–I$_2$/CHCl$_3$: Stock solutions of *HA* (0.3601 g, 13.2×10^{-2} *M*) in chloroform (25 cm^3) and I_2 (0.2072 g, 8.16×10^{-3} *M*) in chloroform (100 cm^3) were used. The following $HA + I_2$ mixtures (in cm^3) were prepared: $0.2+1$, $0.4+1$, $0.6+1$, $0.8+1$, and $1+1$. UV-VIS spectra were obtained in the region (700–250 nm) against chloroform as a blank following the general method above using I_2 in chloroform (8.16×10^{-4} *M*) and *HA* in chloroform (26.4×10^{-4}, 52.8×10^{-4}, 79.2×10^{-4}, 105.6×10^{-4}, 130×10^{-4} *M*).

CHA–I$_2$/CCl$_4$: Stock solution of *CHA* (0.0065 g, 1.8×10^{-3} *M*) in carbontetrachloride (25 cm^3) and I_2 (0.1983 g, 7.81×10^{-3} *M*) in carbontetrachloride (100 cm^3) were used. The following $CHA + I_2$ mixtures (in cm^3) were prepared: $1+1$, $2+1$, $3+1$, $4+1$, $5+1$, and $6+1$. UV-VIS spectra were obtained in the region (700–250 nm) against carbontetrachloride as a blank following the general method above using I_2 in carbontetrachloride (7.8×10^{-4} *M*) and *CHA* in carbontetrachloride (1.8×10^{-4}, 3.6×10^{-4}, 5.4×10^{-4}, 7.2×10^{-4}, 9.0×10^{-4}, 10.8×10^{-4} *M*).

CHA–I$_2$/CH$_2$Cl$_2$: Stock solution of *CHA* (0.0413 g, 11.5×10^{-3} *M*) in dichloromethane (25 cm^3) and I_2 (0.2070 g, 8.16×10^{-3} *M*) in dichloromethane (100 cm^3) were used. The following $CHA + I_2$ mixtures (in cm^3) were prepared: $1+1$, $2+1$, $3+1$, $4+1$, $5+1$, and $6+1$. UV-VIS spectra were obtained in the region (700–232 nm) against dichloromethane as a blank following the general method above using I_2 in dichloromethane (8.16×10^{-4} *M*) and *CHA* in dichloromethane (11.5×10^{-4}, 23.0×10^{-4}, 34.5×10^{-4}, 46.0×10^{-4}, 57.5×10^{-4}, 69.0×10^{-4} *M*).

CHA–I$_2$/CHCl$_3$: Stock solution of *CHA* (0.2477 g, 6.9×10^{-2} *M*) in chloroform (25 cm^3) and I_2 (0.2072 g, 8.16×10^{-3} *M*) in chloroform (100 cm^3) were used. The following $CHA + I_2$ mixtures (in cm^3) were prepared: $0.2+1$, $0.6+1$, $1+1$, $1.4+1$, and $1.8+1$. UV-VIS spectra were obtained in the region (700–250 nm) against chloroform as a blank following the general method above using I_2 in chloroform (8.16×10^{-4} *M*) and *CHA* in chloroform (13.8×10^{-4}, 41.4×10^{-4}, 69.0×10^{-4}, 96.6×10^{-4}, 124.2×10^{-4} *M*).

Computations

Calculations on aniline molecules were performed within the GAUSSIAN 98 [52] Program package. Equilibrium geometries were determined and confirmed by a subsequent calculation of force constants and vibration analysis. Calculations were performed using the closed-shell *Hartree-Fock*, *Becke*'s three parameter density functional theory (DFT) [53] in combination with the *Lee*, *Yang*, and *Parr* correlation functional [54] (B3LYP) and second-order Møller-*Plesset* perturbational method (MP2) [55–59].

Acknowledgement

We are grateful to Prof. *Gottfried Koehler*, Max F. Perutz Laboratories, Department of Chemistry, University of Vienna, Austria, for permitting us to use his account on the Schrödinger II supercomputer of Vienna university for quantum mechanical calculations.

References

[1] Haga N, Nakajima H, Takayanagi H, Tokumaru K (1998) J Org Chem **63**: 5372

[2] Mulliken RS, Person WB (1969) Molecular Complexes: A Lecture and Reprint Volume; Wiley & Sons: New York

[3] Kroll M (1968) J Am Chem Soc **90**: 1097

[4] Dewar MJS, Lepley AR (1961) J Am Chem Soc **83**: 4560

[5] Lippert JL, Hanna MW, Trotter PJ (1969) J Am Chem Soc **91**: 4035

[6] Morokuma K (1977) Accounts Chem Res **10**: 294

[7] Røeggen I, Dahe T (1992) J Am Chem Soc **114**: 511

[8] Matsuo T, Higuchi O (1968) Bull Chem Soc Jpn **41**: 518

[9] Shimkin BM, Triolo AV (1969) Prog ExD Tumor Res **11**: 1

[10] Budni LM, Magadum RS (1992) Spectrochimica Acta A **48**: 1505

[11] Kumar VT, Singh CT, Venkateshwarlu G (2001) Indian J Chem **40**: 622

[12] Bhattacharya S, Baneriee M (2001) Spectrochim Acta **57**: 2409

[13] Bugeanu M, Sahini EmV (1988) Revue Roumaine de Chimie **33**: 75

[14] Csaszar J, Bizony MN (1990) Acta Physica et Chem **36**: 66

[15] Kwon YO, Paek HU, Kim RE (1991) Korean Chem Soc **35**: 343

[16] Kusakawa H, Nishizaki S (1964) Nippon Kajakuzasshi **85**: 241

[17] Andrabi AMS (2002) Indian J Chem **41**: 2306

[18] Sibley PS, Campbell LR, Silber BH (1995) J Phys Chem **99**: 5274

[19] Bhattacharya S, Nayak KS, Chattopadhyay S, Banerjee M, Mukherjee KA (2002) J Phys Chem **106**: 6710

[20] Bertinelli F, Palmieri P, Brillante A, Taliani C (1977) Chem Phys **25**: 333

[21] Bendazzoli G, Bertinelli F, Palmieri P, Taliani C (1976) Chem Phys **16**: 319

[22] Taneja DA, Srivastava PK, Gupta CM (1973) J Chinese Chem Soc (Taipei, Taiwan) **20**: 95

[23] Scheuer-Lamalle B, Durocher G (1976) Canadian J Spectroscopy **21**: 165

[24] Aly AA, Hassann AA, Mohamed SY, Mourad EA, Hopf H (1992) Monatshefte fuer Chemie **123**: 179

[25] Ying B, Hong L (1993) Zhongshan Daxue Xuebao, Ziran Kexueban **32**: 53

[26] Pal P, Saha A, Mukherjee KA, Mukherjee CD (2004) Spectrochim Acta **60**: 167

[27] Tzeng WB, Narayanan K (1998) J Mol Struct **446**: 93

[28] Prasad JV, Rai SB, Thakur SN (1989) Chem Phys Lett **164**: 629

[29] Gough KM, Henry BR (1983) J Phys Chem **87**: 3804

[30] Ahmed MK, Henry BR (1986) J Phys Chem **90**: 1737

[31] Mizugai Y, Katayama M, Nakayama N (1981) J Am Chem Soc **103**: 5061

[32] Dewar MS, Grisdale PJ (1962) J Am Chem Soc **84**: 3539

[33] Lister GD, Tyler JK, Hog JH, Larsen NW (1974) J Mol Struct **23**: 253

[34] Shultz G, Portalone G, Ramondo F, Domenicano A, Hargittai I (1996) Struct Chem **7**: 59

[35] Fukuyo M, Hirotsu K, Higuchi T (1982) Acta Cryst B **38**: 640

[36] Palafox MA, Nunez JL, Gil M (2002) J Mol Struct (Theochem) **593**: 101

[37] Zeng WB, Narayanan K, Shieh KC, Tung CC (1998) J Mol Struct (Theochem) **428**: 231

[38] Vaschetto ME, Retamal BA, Monkman AP (1998) J Mol Struct (Theochem) **468**: 254

[39] Santos L, Martinez E, Ballesteros B, Sanchez J (2000) Spectrochim Acta A **56**: 1905

[40] Kurta M, Yurdakulb M, Yurdakul S (2004) J of Mol Struct (Theochem) **711**: 25

[41] Altun A, Golcuk K, Kumru M (2003) J Mol Struct **625**: 17
[42] Tzeng WB, Narayanan K, Lin JL, Tung CC (1999) Spectrochim Acta **55A**: 153
[43] Sandorfy C (1964) Electronic Spectra and Quantum Chemistry, JN Prentice Hall
[44] Benesi HA, Hildebrand JH (1949) J Am Chem Soc **71**: 1703
[45] Rose NJ, Drago RS (1959) J Am Chem Soc **81**: 6138
[46] Meng-Sheng L, Yun L, Vernon DP, Steve S (2003) J Phys Chem A **107**: 8939
[47] Thompson CC Jr, Demaine PAD (1963) J Am Chem Soc **85**: 3096
[48] Krishna VG, Chowdhury M (1963) J Am Chem Soc **67**: 1067
[49] Furniss BS, Hannaford AJ, Rogers V, Smith PWG, Tatchell AR (1978) ‘‘Text Book of Practical Organic Chemistry’’ 4th edition, Longman Group Ltd
[50] Kubota T (1965) J Am Chem Soc **87**: 458
[51] Krishna VG, Bhowmik BB (1968) J Am Chem Soc **90**: 1700
[52] Frisch MJ, Trucks GW, Schlegel HB, Scuseria GE, Robb MA, Cheeseman JR, Zakrzewski VG, Montgomery JA, Stratmann RE, Burant JC, Dapprich S, Millam JM, Daniels AD, Kudin KN, Strain MC, Farkas O, Tomasi J, Barone V, Cossi M, Cammi R, Mennucci B, Pomelli C, Adamo C, Clifford S, Ochterski J, Petersson GA, Ayala PY, Cui Q, Morokuma K, Malick DK, Rabuck AD, Raghavachari K, Foresman JB, Cioslowski J, Ortiz JV, Baboul AG, Stefanov BB, Liu G, Liashenko A, Piskorz P, Komaromi I, Gomperts R, Martin RL, Fox DJ, Keith T, Al-Laham MA, Peng CY, Nanayakkara A, Gonzalez C, Challacombe M, Gill PMW, Johnson B, Chen W, Wong MW, Andres JL, Gonzalez C, Head-Gordon M, Replogle ES, Pople JA (1998) Gaussian 98, revision A7; Gaussian: Pittsburgh PA
[53] Becke AD (1993) J Chem Phys **98**: 5648
[54] Miehlich BA, Savin HS, Preuss H (1989) Chem Phys Lett **157**: 200
[55] Head-Gordon M, Pople JA, Frisch MJ (1988) Chem Phys Lett **153**: 503
[56] Frisch MJ, Head-Gordon M, Pople AJ (1990) Chem Phys Lett **166**: 275
[57] Frisch MJ, Head-Gordon M, Pople JA (1990) Chem Phys Lett **166**: 281
[58] Head-Gordon M, Head-Gordon T (1994) Chem Phys Lett **220**: 122
[59] Saebo S, Almlof J (1989) Chem Phys Lett **154**: 83